ETEAPOT PTR Benchmark I: Updated Results:

J. D. Talman and R. M. Talman

August 30 , 2023

Abstract

This chapter repeats and updates benchmark lattice investigations first performed using the "all-electric" code ETEAPOT in 2012 for all-electric proton EDM rings. Recently introduced is the extension to "predominantly electric bending"; this extension has not influenced this PTR Benchmark I. The lattice electric bending fields for three PTR files have field shape indices $m = 0.19447, 0.29447, 0.32349, 0.39447$. Values of horizontal and vertical tunes, and beta functions at the origin (midway between adjacent bends) are tabulated. Results are compared to values obtained from a linearized transfer matrix formalism.

1 Introduction

All-electric lattices for a storage ring to measure the electric dipole moment (EDM) of the proton, now generalized to support the superposition of weak magnetic bending to enable storage ring measurement of nuclear transmutation, are described in a CERN Yellow Report, CERN-2019-001-M, "Feasibility Study for a Storage Ring to Search for EDMs of Charged Particles". Earlier designs were contained in a BNL proposal by the Storage Ring EDM Collaboration, *A Proposal to Measure the Proton Electric Dipole Moment with* 10^{-29} *e-cm Sensitivity*[1]. The lattices studied here have been stripped down to their bare essentials in order to simplify benchmark comparisons of various simulation codes. All results use ETEAPOT, as described in an (unpublished) 2012 benchmark report (to the DOE, in connection with their financial support at the time). They are replicated using (updated) ETEAPOT in the present report.

An electric field with index m power law dependence on radius r for y=0, is

$$\mathbf{E}(r,0) = -E_0 \frac{r_0^{1+m}}{r^{1+m}} \hat{\mathbf{r}}, \tag{1}$$

and the electric potential $V(r)$, adjusted to vanish (on the storage ring design orbit) at $r = r_0$, is

$$V(r) = -\frac{E_0 r_0}{m}\left(\frac{r_0^m}{r^m} - 1\right). \tag{2}$$

By convection E_0 is positive, even though the electric field applies centripetal force to all nuclear isotopes including the proton.

The "cleanest" case theoretically has m=1, in which case the field is known as the Kepler or the Coulomb electric field. Our problem is a bit more general than this nonreletivistic terminology suggests, since our treatment is necessarily relativistic. For m=1 the Kepler problem can be solved with the same generality in the relativistic as in the nonrelativistic case. However, the orbits are no longer exactly elliptical, nor exactly closed [3].

The full rings simulated in this chapter are circular and consist of eight octants, each containing a single almost identical half cell. A single bending element , with toroidally-shaped electrodes is shown in perspective in Figure 2. Also shown in the figure, though not used in this benchmark I report, are coils for superimposing magnetic field. For field index m=0 the electrodes are concentric cylinders. For m=1 the electrodes would be concentric spheres. The most promising behavior is expected to lie in the range $0.1 < m < 0.45$.

A PTR lattice layout is shown in Figure 1. Optics for one quadrant (with arc length parameter s taken as a Cartesion straight line coordinate) are shown on the left. One quadrant of the same lattice is shown in perspective view in Figure 1.

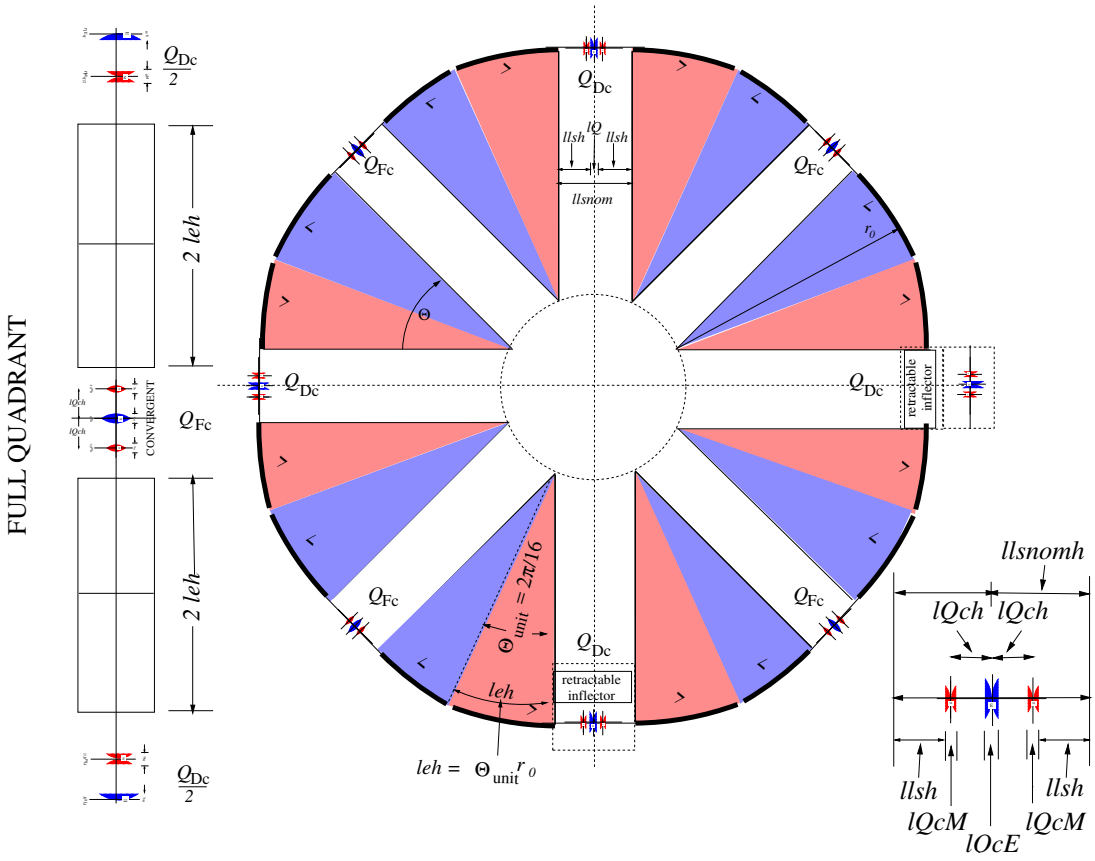

Figure 1: Lattice layouts for PTR, the proposed prototype nuclear transmutation storage ring prototype; The circumference has been taken to be 102 m, but the entire lattice can be scaled, e.g. to reduce peak field requirements. "Compromise" quadrupoles (shown lower on the right) are located in each of eight long straight sections. Detailed lattice files can be downloaded from GIT.

For m=0 the fields are independent of vertical displacement y, which implies that there is no vertical focusing provided by the bending field. Provision of vertical stability therefore requires focusing quadrupoles; they are labeled q in Figure 1. As well as being required for vertical stability, the q quadrupoles are the only elents available in the control room for adjusting the optics of the storage ring.

2 Parameters of Benchmark Lattices

Lattice description files, with names like `PTR_m_nom=0.32349-sl4.sxf`, readable by accelerator programs such as MAD or ETEAPOT, (and consistent with MAPLE parameterization of the same lattices) are located in the "data" directory. These SXF lattice files are produced in `/home/oxygen/XML2ADXF` and `/home/oxygen/ADXF2SXF`. Their (abbreviated) filenames are column headings in Table 1, which contains lattice parameters and lattice properties such as tunes and beta functions determined by ETEAPOT. For example, a related full lattice name is "PTR_m_nom=0.29447-sl4.sxf". (The circumference is always

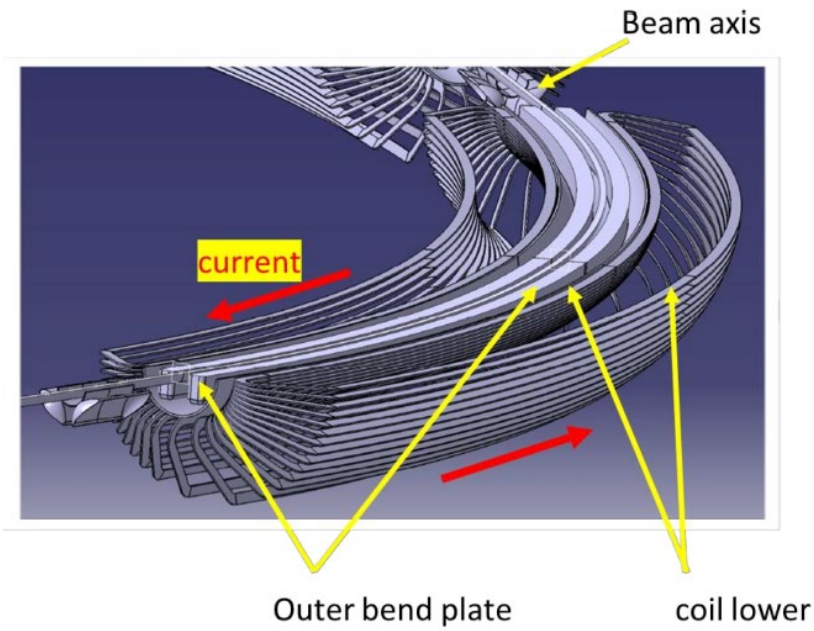

Figure 2: Perspective mock-up of one sector of PTR, the superimposed E/M prototype ring. "Short-circuited end" $\cos\theta$-dipoles surround the beam tube, within which are the toroidal capacitor plate electodes. No magnetic field is superimposed in this benchmark.

contained in the final line of the lattice ".sxf" file.) Later the ETEAPOT lattice prperties are to be compared with the same properties calculated by MAPLE.

3 Twiss Parameter Extraction

A once-around ("monodromy" in mathematical terminology) transfer matrix at any point in the ring has the standard Twiss parameterization,

$$\mathbf{M} = \begin{pmatrix} \cos\mu + \alpha\sin\mu & \beta\sin\mu \\ -\frac{1+\alpha^2}{\beta}\sin\mu & \cos\mu - \alpha\sin\mu \end{pmatrix}. \tag{3}$$

At a mirror symmetry point in the lattice, as at present, though not in general, α vanishes. The phase advance $\mu = 2\pi Q$ can be obtained from

$$\cos\mu = \frac{M_{11} + M_{22}}{2}, \quad \text{and} \quad M_{12} = \beta\sin\mu. \tag{4}$$

This has assumed that β is, by definition, positive. These equations determine the signs of both $\cos\mu$ and $\sin\mu$. Reading counter-clockwise, the four consecutive phase space quadrants, I/II/III/IV, are characterized by cosine, sine sign pairs ++/-+/- -/+-, respectively. We then obtain the fractional parts of the phase advance from

$$\mu = \begin{cases} \cos^{-1}(\frac{M_{11}+M_{22}}{2}), & \text{if quadrant is I or II} \\ 2\pi - \cos^{-1}(\frac{M_{11}+M_{22}}{2}), & \text{if quadrant is III or IV} \end{cases}. \tag{5}$$

	variable name	unit	PTR_m=0.29447	m=0.32349	m=0.39447
cells/arc	NCellPerOctant		1	1	1
bend radius	r0	m	11.0	11.0	11.0
long drift length	llsnom	m	4.14214	4.14214	4.14214
half bend of cell	lh	r	$2\pi/16$	$2\pi/16$	$2\pi/16$
half bend length	leh	m	$2\pi r0/16$	$2\pi r0/16$	$2\pi r0/16$
circumference	circum	m	102.252179	102.252179	102.252179
inverse focal length	delq	1/m	-0.009091	-0.009091	-0.009091
field index	m		0.29447	0.32349	0.39447
horizontal beta	betax	m			
vertical beta	betay	m			
horizontal tune	Qx				
vertical tune	Qy				

Table 1: Parameters of benchmark PTR lattices, and Twiss parameters (i.e. dynamic properties) calculated by ETEAPOT using linearized transfer matrices. Note that ETEAPOT always "slices" each bend in the "sxf" file in half, before propagating sequentially through both slices. This makes properties available at the bend center.

This still only partially resolves the aliasing ambiguity. Resolving the integer tune ambiguity requires keeping track of phase space quadrants while tracking through the lattice. To avoid error in this process it is important for sampling intervals small enough that no phase quadrant can be skipped. This keeping track of the integer tune is indicated in captions to graphs below. We then obtain β from Eq. (4), and α from

$$\alpha = \frac{M_{11} - M_{22}}{2 \sin \mu}. \tag{6}$$

It is because the TEAPOT family of codes use only particle tracking, and no transfer matrices in studying ring behavior—transfer matrix components, and Twiss and other lattice functions are only obtained for the purpose of comparing results with more conventional accelerator simulation codes.

4 ETEAPOT tune determinations and analytic comparisons

4.1 Data collection organization

In all cases, $m = 0.29447, 0.32349, 0.39447$, the lumped Q-quadrupoles strengths, $delq$, were adjusted to a "nearly-off" state, just strong enough to produce vertical stability in all cases. For each of the three benchmark lattices, bunches of 21 standard particles are tracked for ten turns. Each of the bend elements is sliced in half for this (and all other) analyses. The graphs show horizontal and vertical displacements for two of the standard particles at the exits from each turn. Both transverse tune determinations are shown in the figure captions.

The reason for tracking a significantly large number of turns (10), is to avoid "aliasing" problems which will be explained later.

Once-around transfer matrices are obtained from the 21 standard particles using numerical differences. This differencing is based on the smallness (typically 1 μm spatial displacement, 1 μr angular displacement) of the initial offsets. Sensitivity to this choice has been investigated previously. Twiss parameters, β_x, β_y, and μ_x, μ_y are calculated using the procedures already described. The fractional and integer tune values are obtained from the graphs.

Each bend element in any SXF lattice description file corresponds to a single bend element in an actual ring and is therefore referred to as a "single bend". By the internal construction of ETEAPOT, each such bend is sliced at least once, and (optionally) more times.

4.2 PTR lattice tracking tune determinations

The following figures exhibit the determination of horizontal and vertical tunes Q_x and Q_y for each of the three lattices under study, by counting the number of betatron oscillations occuring after ten complete revolutions. The arithmetic is completed in the figure captions. Table 2 shows the lattice parameters obtained with $m = 1$, "spherical" bend-

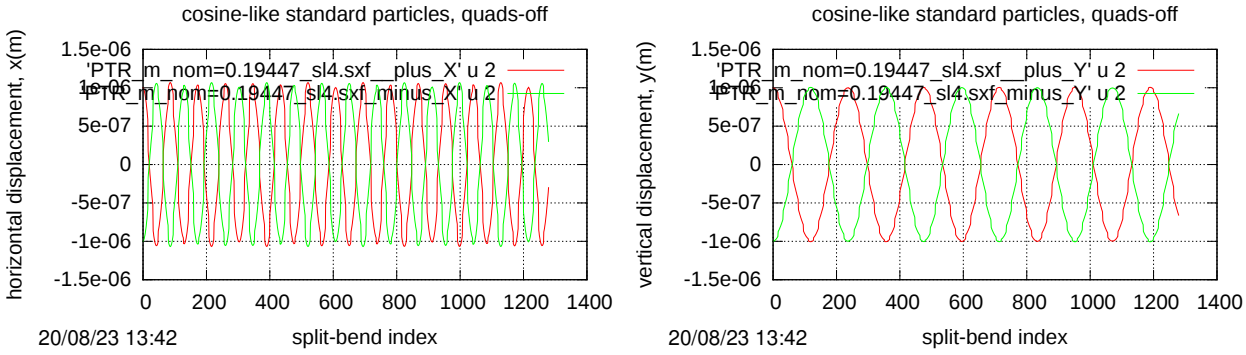

Figure 3: Lattice `PTR_m_nom=0.19447-sl4.sxf`; Upper: horizontal Displacement: 10 turns, 1 sample per split bend; $Q_x \approx 15.2$ osc/10turns=1.52 osc/turn; the horizontal tune is Q_x= 1.52. Lower: vertical Displacement: 10 turns. $Q_y \approx 5.4$ osc/10turns=0.54 osc/turn. The vertical tune is Q_y= 0.54.

ing, with minimal ETEAPOT slicing of 2 slices per bend. ETEAPOT results agree well with analytic lattice calculations using MAPLE. The accuracy of "differentiation by differencing" is investigated. The effect of increasing the unit differencing value `tiny` $= 10^{-6}$ by two orders of manitude has negligible effect on the lattice parameters, showing that the differencing provides sufficient accuracy.

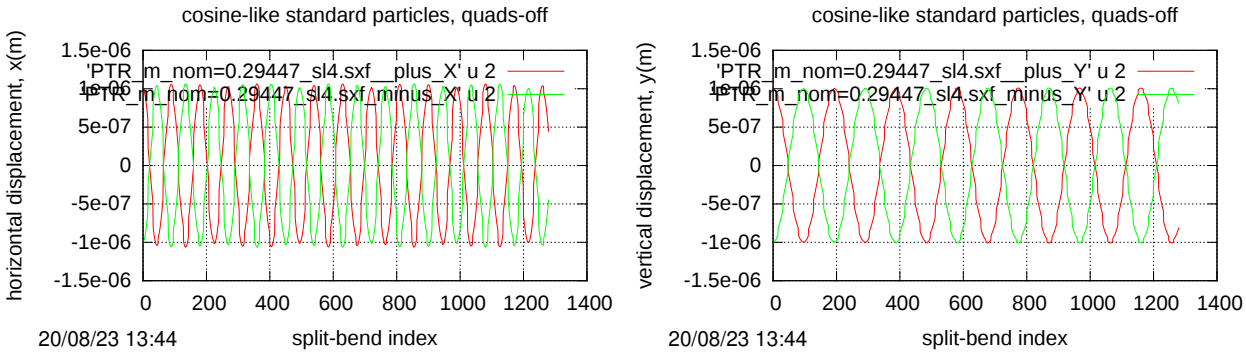

Figure 4: Lattice `PTR_m_nom=0.29447-sl4.sxf`; Upper: horizontal Displacement: 10 turns, 1 sample per split bend; $Q_x \approx 14.2$ osc/10turns=1.42 osc/turn; the horizontal tune is Q_x = 1.42. Lower: vertical Displacement: 10 turns. $Q_y \approx$6.55 osc/10turns=0.655 osc/turn. The vertical tune is Q_y = 0.655.

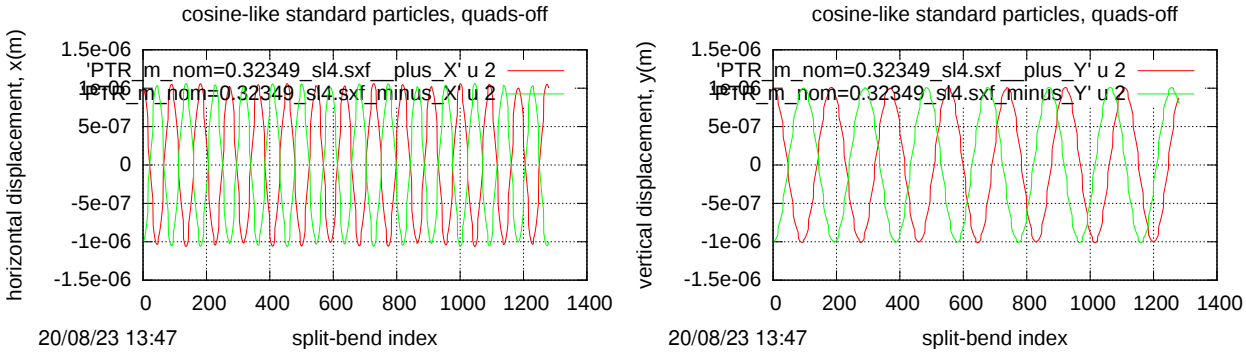

Figure 5: Lattice `PTR_m_nom=0.32349-sl4.sxf`; Upper: horizontal Displacement: 10 turns, 1 sample per split bend; $Q_x \approx 14.0$ osc/10turns=1.40 osc/turn; the horizontal tune is Q_x = 1.40. Lower: vertical Displacement: 10 turns, 1 sample per split bend. $Q_y \approx$6.55 osc/10turns=0.655 osc/turn. The vertical tune is Q_y = 0.655.

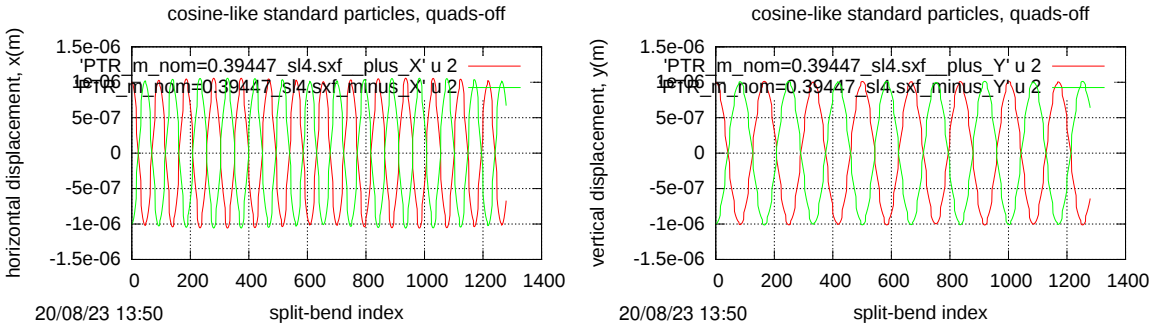

Figure 6: Lattice `PTR_m_nom=0.39447-sl4.sxf`; Upper: horizontal Displacement: 10 turns, 1 sample per split bend; $Q_x \approx 13.55$ osc/10turns=1.355 osc/turn; the horizontal tune is Q_x = 1.355. Lower: vertical Displacement: 10 turns, 1 sample per split bend. $Q_y \approx 7.6$ osc/10turns=0.76 osc/turn. The vertical tune is Q_y = 0.76.

program			MAPLE	ETEAPOT	MAPLE	ETEAPOT	MAPLE	ETEAPOT
field index	m		0.29447	0.29447	0.32349	0.32349	0.39447	0.39447
horizontal beta	`betax`	m						
vertical beta	`betay`	m						
horizontal tune	`Qx`			1.42		1.40		1.355
vertical tune	`Qy`			0.655		0.655		0.76

Table 2: Comparison of ETEAPOT and MAPLE tune results. Spaces left blank are to be filled in in subsequent benchmark tests, which will also produce more acccurate values. All numerical differentiation displacements in ETEAPOT are takn to be `tiny`=10^{-6} m.
. The calculational parameter "`tiny`" can be increased by at least two orders of magnitude without changing the results significantly.

5 Comments and Conclusions

ETEAPOT tracking was initially based on an analytical relativistic astronomical Kepler planetary orbit formulation of Munoz and Pavic, listed along with other relevant formulations in the bibliography below. Since this analytic approach was quite unwieldy it was eventually replaced more in the pirit of the original TEAPOT code. The introduction of superimpoed magnetic bending rules out any cloed form analytic approach.

We refer to ETEAPOT orbit tracking as representing a "Schrödinger Picture" determination of beam evolution in a storage ring. Calculated using classical (relativistic) mechanics, in a wave-like picture of particle evoluting with s, these "eikonal curves", calculated as in geometric optics, are orthogonal to wavefronts in a Schrödinger wave propogation picture. These rays can be used to calculate lattice beta functions as "ray envelopes" in following benchmark investigations.

The (MAPLE) BSM code treats the beam transfer matrices, whose elements are expressed in terms of beta functions. as evolving with s in a "Heisenberg-like" picture

FOLLOWING is NOT YET UPDATED to PTR lattice

For the $m = 1$ case, there is nearly exact agreement between the linearized analytic formulae and the tracking formalism. This is "as should be", but far from automatic. The equations of the linearized transfer matrix formalism and the arbitrary-amplitude Munoz-Pavic seem utterly different. So the close agreement confirms *both* approaches. This comment mainly applies to the "in-plane" horizontal motion. Agreement of the "out-of-plane" vertical motion, where the overall agreement is less impressive, especially as investigated with a pre-sliced SXF lattice, in Sections **??** and **??**. Vertical steering errors, however small, are amplified by the weak vertical focusing of the lattice.

The agreement for $m \neq 1$ is excellent, but clearly not as good as for $m = 1$. This strongly suggests that the (artificial) perturbative kick compensation is not quite perfect. It is also not surprising that the deviation is proportional to $(m-1)^2$; and that, for $m = 1$, the kick correction strength vanishes.

For most practical purposes, the code performance in the parameter range $-1 \leq m \leq 1$ has been shown to be satisfactory.

References

[1] Storage Ring EDM Collaboration, *A Proposal to Measure the Proton Electric Dipole Moment with* 10^{-29} *e-cm Sensitivity,* especially Appendix 1. October, 2011

[2] C. Møller, *The Theory of Relativity,* Clarendon Press, Oxford, 1952,

[3] G. Muñoz and I. Pavic, *A Hamilton-like vector for the special-relativistic Coulomb problem,* Eur. J. Phys. **27**, 1007-1018, 2006

[4] R. Talman, *Geometric Mechanics,* John Wiley and Sons, 2000

[5] J. Aguirregabiria et al., Archiv:physics/0407049v1 [physics.ed-ph] 2004,

[6] U. Torkelsson, Eur. J. Phys., **19**, 459, 1998,

[7] T. Boyer, Am. J. Phys. **72** (8) 992, 2004